Interference Analysis and Mitigation for UAV Communications in Drone Corridors

Cameron Ellis, Minglong Zhang and Vuk Marojevic
Department of Electrical and Computer Engineering, Mississippi State University, USA
Email: {ce731, mz354, vuk.marojevic}@msstate.edu

2023 26th International Symposium on Wireless Personal Multimedia Communications (WPMC) | 979-8-3503-0890-7/23/$31.00 ©2023 IEEE | DOI: 10.1109/WPMC59531.2023.10338970

***Abstract*—Unmanned aerial vehicles (UAVs) have witnessed widespread adoption in the modern world, with their development set to continue into the future. As UAV technology and applications advance, it becomes imperative to understand their communication capabilities. UAVs experience distinct radio propagation conditions compared to ground-based radio nodes, necessitating a critical investigation into aerial radio node performance. This paper analyzes interference in UAV-to-UAV (U2U) communications within drone corridors and proposes an interference mitigation strategy utilizing millimeter wave (mmWave) beamforming. Employing a semi-persistent scheduling approach from the Third Generation Partnership Project (3GPP) sidelink communications for low altitude aerial nodes in drone corridors, the study primarily examines interference from drone clusters within designated air corridors. To assess U2U communication performance, a 3GPP standard-compliant cross-layer simulator is developed. Simulation results demonstrate that employing mmWave beamforming instead of isotropic transmission substantially reduces interference, leading to higher communications reliability and enabling more UAVs to occupy and communicate in the airspace.**

Keywords—Drone corridors, mmWave, Beamforming, Interference mitigation, 5G NR V2X.

I. Introduction

Unmanned aerial vehicles (UAVs) have gained significant popularity in the commercial sector, attracting numerous companies eager to harness this evolving technology. The unparalleled flexibility of UAVs allows for a diverse array of applications and use cases. They prove invaluable in supporting intelligent transportation systems through traffic monitoring, accident reporting, and efficient aerial delivery of cargo and medication, among other vital functions [1]. Moreover, UAVs find utility in aiding farmers with crop management, collecting remote sensor data, facilitating search and rescue missions, disaster recovery operations, and enhancing terrestrial communications [2], [3].

As the popularity of drones arises and the airspace becomes increasingly crowded, the imperative to explore radio interference mitigation techniques becomes apparent. However, unlike ground-based nodes, aerial nodes benefit from elevated positions, resulting in frequent line-of-sight (LoS) channels not only to the intended target but also to unrelated nodes. Consequently, this causes an excessive radio frequency (RF) footprint, causing interference challenges. Given the unique nature of aerial nodes, traditional interference mitigation techniques tailored for ground-based scenarios may be ineffective when dealing with the more severe UAV interference. Particularly, aerial nodes employing isotropic antennas encounter interference among themselves, further impacting nodes over a larger area in comparison to terrestrial communications.

To address these challenges, numerous researchers advocate the implementation of drone corridors, reminiscent of terrestrial highway systems, encircling specific areas. These corridors offer a structured framework for regulating and closely monitoring commercial UAVs, while also taking into account residential privacy concerns and potential interference with existing commercial aircraft traffic [4]. Notably, these proposed corridors not only span across smaller regions but also enable long-range traversal between cities and over rugged terrains, ensuring predictability in drone operations [5].

As the use of drone corridors becomes more prevalent over areas without a central network, U2U communication capabilities will be needed. Standards for this communication scheme are being proposed by 3GPP [6]. A 3GPP Technical specification [7] defines the essential requirements for providing unmanned aircraft system (UAS) services through the ad-hoc mode of the vehicle-to-vehicle (V2V) communication networks. Technical report [8] and [9] identify the network infrastructure and the application architecture to support UAV-enabled applications. The International Telecommunication Union (ITU) and the IEEE provide complementary standards for UAV applications and use cases [10], [11].

The interference caused by aerial U2U communications can manifest over long distances, even at relatively low aircraft densities, owing to the absence of physical obstructions in the airspace. This paper addresses this challenge by proposing a solution that implements millimeter wave (mmWave)-based beamforming for UAV communications within drone corridors. Our contributions encompass a comprehensive analysis of the interference in U2U communications, the development of a tailored open-source simulation platform for an advanced U2U network utilizing the 5G New Radio (NR) vehicle-to-everything (V2X) protocol, and the execution of numerical analysis to evaluate the effectiveness of the proposed scheme.

The rest of the paper is organized as follows. The next section of this paper describes related works in this area including utilization of beamforming. Section III describes the system model, formulates the problems and provides a solution based on analysis. It is followed by the simulator and experimental design in Section IV. Section V presents and discusses the results from the simulations and Section

VI provides the concluding remarks.

II. Prior Work in UAV Communications

Researchers in [12] propose a novel solution for devising base station placement while leveraging mmWave technology in order to meet the necessary quality of service (QoS) requirements. This paper uses beamforming however it is employed to improve the signal attenuation issues faced by the researchers and not for traffic mitigation or spectrum reuse purposes. Many works that have studied beamforming focus on terrestrial networks that are not suited for drone based networks. A cellular tower will for example always be at a fixed location and lack the dynamic movement of a UAV based platform. Shi *et al*. [13] designed a prototype testbed which implemented UAV based beamforming using a Universal Software Radio Peripheral (USRP) based software defined radio (SDR). The researchers also developed an IEEE 802.11 mechanism to support channel feedback that is needed for the beamforming operations. They focused on the communication link between a stationary terrestrial node and a beamforming capable UAV whereas our paper studies the interference mitigation between multiple beamforming capable UAVs in a drone corridor.

Many papers also focus on the opposite approach which is transmission from an aerial node to a terrestrial node. Akram Al-Hourani *et al*. [14] sought to develop a statistical propagation model for predicting air-to-ground pathloss between a low altitude platform (LAP) and a terrestrial terminal. In this case the researchers aimed to minimize the path loss between an aerial node and a terrestrial node. Low altitude platforms are typically defined as quasi-stationary aerial platforms with an altitude below ten thousand meters. This means that the aerial nodes are intended to hover or float in the same general area while communicating with the ground. Our paper differs from this approach by simulating highly mobile aerial nodes that move freely over great distances within the corridor. The researchers also specified that they focused on LAPs located at altitudes between two hundred meters and three thousand meters whereas our approach uses aerial nodes in closer proximity with an altitude below three hundred meters.

III. System Design

A. Network Model

We consider a U2U communication network consisting of $\mathcal{K}$ parallel drone corridors. The corridors are evenly distributed with distance of S for each two adjacent corridors. For a corridor i ($1 \leq i \leq \mathcal{K}$), there are N_i UAVs flying with a constant velocity V. The drones in each corridor are separated by distance D. We let U_j^i denote the j-th UAV in corridor i.

Drone corridors serve as aerial highways, providing a structured airspace framework for UAVs. Each UAV within these corridors is equipped with a radio device that facilitates communication with other UAVs, sharing crucial data such as position, heading, speed, and other relevant information. This communication fosters enhanced flight safety and efficient traffic flow. Utilizing the 5G New Radio (NR) sidelink communication channel, both flight-related and user-related data can be efficiently exchanged. Flight-related information encompasses fundamental safety messages akin to modern terrestrial vehicle-to-everything (V2X) communications, contributing to the seamless operation of UAVs within the designated airspace.

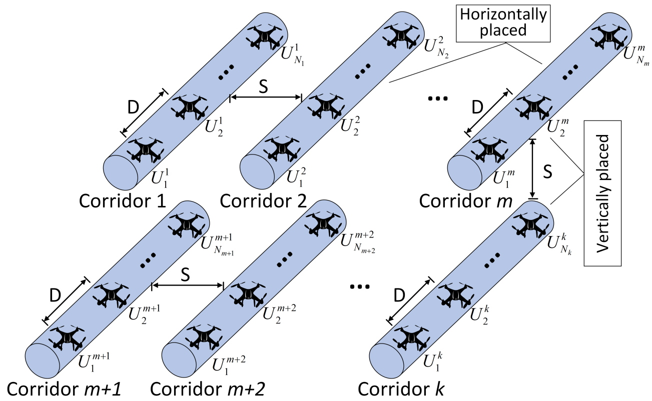

Fig. 1: Radio radiation graph for directional transmission and reception.

To facilitate the dissemination of the flight-related or user-related information, we design an advanced communications network with focus on the physical and medium access control layers. Specifically, we leverage the 5G NR V2X Mode 2 communications protocol, where vehicles send broadcast or unicast messages to other vehicles without requiring network infrastructure. A main characteristic of Mode 2 communications is the semi-persistent scheduler which is employed by each vehicle to find a suitable resource to transmit [15]. In the designed network, U2U communications are conducted along drone corridors.

In the proposed network, for a U_j^i in the corridor i, it concerns about the UAV in front and behind, i.e., U_{j-1}^i and U_{j+1}^i ($(1 \leq j \leq N_i - 1)$), respectively, since they all fly along the same one-way corridor.

Distinguished from the terrestrial V2X communications, U2U communications in the network maintain a line-of-sight (LoS) scenario for the recipients, which may lead to less path loss and higher reception probability. However, on the other hand, due to the same reason, other transmitters from the same or different corridors can inevitably cause severe interference. In this paper, we aim to investigate this issue and propose a solution to reduce the interference thus enhancing a high signal-to-interference-plus-noise ratio (SINR). The SINR at a receiving node U_{j+1}^i can be expressed as

$$SINR_{U_j^i} = \frac{E_s G_{U_j^i}^{U_k^i}}{\sum_m \mathcal{I}_m + P_{N0}} (k \neq j), \tag{1}$$

where P_{N0} is the noise power, E_s is the transmission power, $G_{U_j^i}^{U_k^i}$ is the channel gain between the sender U_k^i and the receiver U_j^i (so the reception power $P_{rx} = E_s G_{U_j^i}^{U_k^i}$), and $\mathcal{I}_m$ is the interference power from node m.

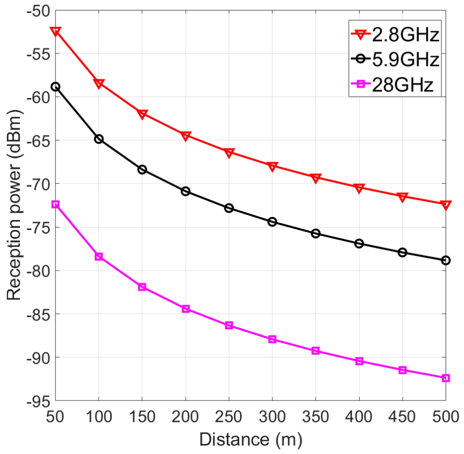

Fig. 2: Reception power for isotropic transmission and reception.

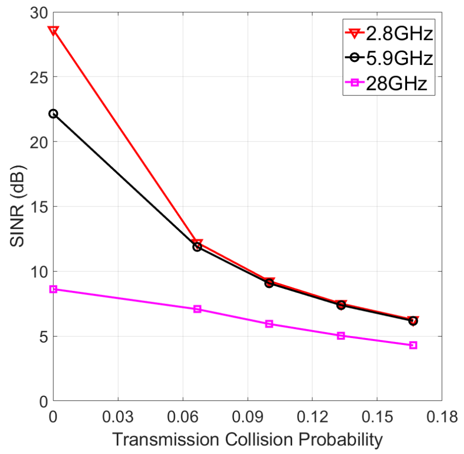

Fig. 3: SINR at a reception node against diverse transmission collision probabilities (bandwidth = 50 MHz).

B. Problem Formulation and Interference Analysis

To enhace the SINR at a receiving node, the most effective way is to reduce the sum of the interference power as shown by (1). The reception power P_{rx} can be calculated by

$$P_{rx} = E_s G_{tx} G_{rx} f_{pl}(d, f_c), \tag{2}$$

where G_{tx} and G_{rx} is transmission and reception gain, respectively, and $f_{pl}(\cdot)$ represents the pathloss function that is conditional to distance d and carrier frequency f_c. The channel gain in (1) $G_{U_j^i}^{U_k^i} = G_{tx} G_{rx} f_{pl}(d, f_c)$ because the small-scale fading is ignorable in U2U-communication situations. Owing to this property of the U2U communications in the system model, a free-space channel model is used to approximately obtain the reception power P_{rx} or the interference power $\mathfrak{I}_m$. According to Frii's channel model, if isotropic transmission and reception are adopted in the U2U communications, the reception power is

$$\begin{aligned} P_{rx} =& E_s G_{tx} G_{rx} \left(\frac{\lambda}{4\pi d} \right)^2 \\ =& E_s G_{tx} G_{rx} \left(\frac{c^2}{4\pi {f_c}^2} \right) \left(\frac{1}{4\pi d^2} \right), \end{aligned} \tag{3}$$

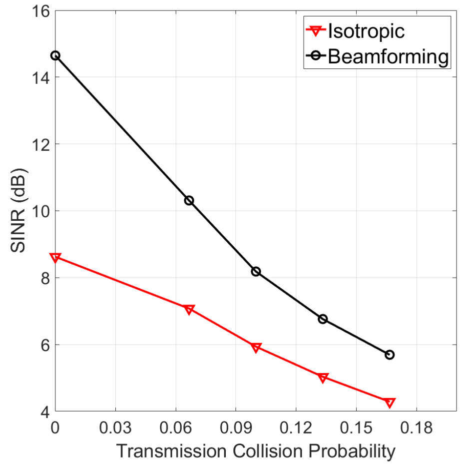

Fig. 4: SINR comparison between isotropy and beamforming at various transmission collision probabilities (bandwidth=50 MHz, f_c = 28 GHz).

where c is the speed of light, λ is the wavelength and d is the distance between transmitter and receiver. In the above equation, the term $(\lambda/(4\pi d))^2$ can be deemed as the pathloss, while $c^2/(4\pi {f_c}^2)$ is the aperture size for isotropic reception.

Based on (2) and (3), Fig. 2 evaluates the reception power against the distance for U2U communications, where the transmission power is 23 dBm. Evidently, with the same distance, higher carrier frequency will result in higher pathloss, because the reception power declines if the carrier frequency becomes higher.

To showcase how transmission collisions affect SINR in U2U communications, a U2U network with 3 parallel corridors is investigated. The parameters of the network are $\mathcal{K} = 3$, $N_1 = N_2 = N_3 = 20$ (i.e., 20 UAVs in each corridor), and $D = 100$. Among total 30 transmitter-receiver pairs, we calculate the SINR at the recipient node U_2^{12} given U_2^{11} is the transmitter. Node U_1^7, U_1^{15}, U_3^7 and U_3^{15} are selected to yield interference. Fig. 3 shows that with the increase of transmission collisions, lower SINRs are observed, regardless of whichever frequency adopted, and more interestingly, the mmWave case (e.g., 28 GHz) has less affection than the other two cases, because its SINR curve does not drop as dramatically as the other two.

From the above phenomena, it is inspired that we can use mmWave to reduce the effect of low SINR caused by transmission collisions. Meanwhile, to cope with the large pathloss resulted from high frequency, beamforming and transmission/reception antenna array are leveraged at the same time. Multiple reception antennas can effectively increase aperture size, thereby increasing the received power. Beamforming can reduce the interference level at a target receiver. This is clearly validated by Fig. 4, which compares the SINR at a reception node between the isotropic and the beamforming transmission. With the same configuration in node selection as in Fig. 3 but employing a 2×2 antenna array to increase the aperture size, the obtained SNR (i.e., the case of zero transmission collision) of the beamforming scheme is 6 dB higher than that of the isotropic scheme. The curve representing beamforming still maintains higher SINR even with the existence of interference.

C. Interference Mitigation by Beamforming

From the above analysis, in order to mitigate the interference in U2U communications, we propose employing mmWave beamforming instead of isotropic transmission and reception. Because the flight paths are structured, beamforming can limit the RF footprint of aerial node transmissions, and thus lowering the interference when the aerial network becomes congested.

In the proposed mmWave beamforming scheme, all the drones are equipped with a beamforming antenna array. Each array consists of four antenna elements. The elements are arranged into a 2x2 uniform planar array. This allows for the digital steering of the beam as opposed to using mechanical solution such as a directional antenna mounted on a gimbal. The beamforming vector is calculated with the consideration for both azimuth and elevation differences.

The azimuth angle of the vector that spans between a given transmitter (TX) and receiver (RX) drones by taking the inverse tangent of the x and y components of the vector between them is calculated by

$$\theta_{xy} = \tan^{-1}(V_y/V_x), \tag{4}$$

where V_x and V_y are speed components along x and y axis, respectively. The elevation angle between a given pair of drones is obtained by

$$\varphi_z = \cos^{-1}(V_z/V_L), \tag{5}$$

where V_z is the component of the z component, and V_L is the distance between the TX-RX pair. The calculations are carried out for each frame of the simulation so that the beamforming vectors are constantly aligned with their moving targets.

IV. Simulator and Experiment Design

In order to test the effectiveness of the proposed U2U beamforming scheme, a simulator is developed leveraging the Network Simulator NS-3. Traffic scenarios are created in Simulation of Urban Mobility (SUMO) to handle large networks. The UAVs are initially modeled as cars as SUMO does not naively support aerial vehicles. This is resolved in later steps by modifying the outputted z coordinate of the cars that is typically used for differences in terrestrial elevation and setting it to the desired altitude. After the corridors are modeled in SUMO, the network is saved and vehicles are added and given specific speeds and directions.

After the vehicle corridors and routes are created, the SUMO output files are imported into the NS-3 framework. These files are utilized to create a mobility model. The NS-3 model features a full V2V protocol stack of 5G NR. To make the simulation more realistic, the pathloss model used for the simulation is based on [16]. The pathloss equations in dB for line of sight (LOS) or non-LOS applications are

$$f_{pl}(d, f_c) = 32.4 + 20log_{10}(d) + 20log_{10}(f_c) \text{ or } \tag{6}$$

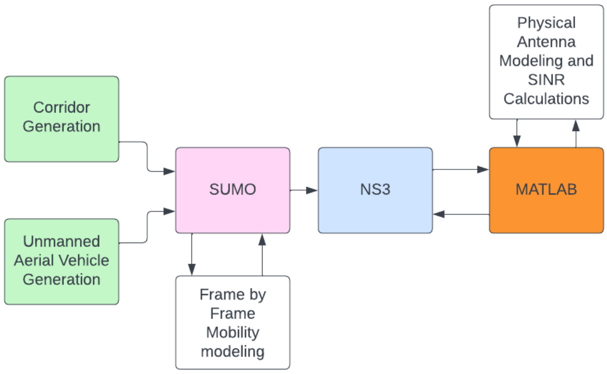

Fig. 5: The structure of the simulation system designed for the U2U networks.

$$f_{pl}(d, f_c) = 36.85 + 30log_{10}(d) + 18.9log_{10}(f_c), \tag{7}$$

respectively. We assume that U2U communications maintain LOS throughout the entire simulation. In the simulations, the SINR measured in logarithmic units (dB) during a given simulation frame is obtained by

$$SINR = 10log_{10}\left(\frac{\int \mathcal{R}_{psd}(f)df}{\sum_m \left(\int \mathcal{I}^m_{psd}(f)df\right) + BN_{psd}}\right), \tag{8}$$

where $\mathcal{R}_{psd}(\cdot)$ (or $\mathcal{I}^m_{psd}(\cdot)$) represents the power spectral density for the received signal (or the interference caused by an interfering node m), N_{psd} is the noise power spectral density, and B is the bandwidth.

The SINR is acquired every 10 ms by pausing the simulation temporarily and exporting the positions of all vehicles into a MATLAB program that calculates the antenna propagation patterns in the 3D space. This information is then fed back into NS3 which then steps the simulation forward another 10 ms. Fig. 5 shows the design diagram of the system simulator. It is worth noting that all scenarios utilize the same communication scheme including regardless of antenna configuration.

The series of experiments focuses primarily on three scenarios. The first scenario features two corridors placed . In this scenario the two corridors are placed one hundred meters apart horizontally with distance $S = 100$ m. In each corridor, $N_1 = N_2 = 10$. A drone within each corridor is spaced one hundred meters apart from the drone in front of and behind it. Initially the two groups of drones are facing towards each other with a one thousand meter gap between the lead drone in each corridor. Upon simulation start each drone moves down its respective corridor at 6 m/s. After spanning the one thousand meter initial gap the two groups of drones pass each other while remaining in their respective corridor.

Scenario 2 is set up similarly to scenario 1 but with the two drone corridors arranged vertically. The number of drones, their spacing, and their velocity remain the same as in the previous scenario. In scenario 3, the two drone corridors are spaced farther apart at three hundred meters. This scenario

TABLE I: Three configurations in drone corridor design

	Scenario 1	Scenario 2	Scenario 3
Horizontal UAV spacing within corridor D	100 m	100 m	100 m
Vertical UAV spacing within corridor	0 m	0 m	0 m
Vertical spacing between corridors S	0 m	100 m	0 m
Horizontal spacing between corridors S	100 m	0 m	300 m
UAV Velocity V	6 m/s	6 m/s	6 m/s
Antenna array	2×2 Planar	2×2 Planar	2×2 Planar
Number of UAVs per corridor N_i	10	10	10

was designed to show the advantage of using directional antennas not only for interference mitigation between corridors as in the other scenarios but also to study the advantage within a single drone corridor.

In each of the three scenarios, the antennas mounted on the drones are configured in one of two ways. In the first setup, all drones are equipped with isotropic antennas, while in the second setup, directional antenna arrays for beamforming are deployed. Throughout all scenarios, the communications are operated at the 28 GHz band.

Regarding each scenario, SINR values are acquired during the experiments adopting one of two setups above, thus enabling the direct comparison of the interference mitigation effect between the isotropic antennas and the directional antennas. Table 1 captures the key experimental parameters in the simulations.

V. Simulation Results

To show the level of the interference in an intuitive way, Fig. 6 depicts the radio footprint in a two-corridor UAV network. It compares the radiation pattern of radio waves for both isotropic transmission and beamforming. One might notice that the antenna patterns are asymmetrical, this is the result of vibrations within the antenna mount being generated within the simulation. It was critical to account for these vibrations as they can effect the transmission significantly and would occur in the real world. Evidently, applying isotropic antennas results in higher interference level from neighbouring transmitters. By contrast, beamforming with directional antennas reduce the interference.

Fig. 7 plots the collected SINR values versus time for all three scenarios. The SINRs are relatively high at first as the two groups of drones initially have one thousand meters of separation distance. As the two groups of ten drones each approach each other the SINR decreases as more interference is present. The isotropic (marked as Omni in the figure) and beamforming (marked as Dir. in the figure) antenna configuration of Scenario 1 has the lowest average

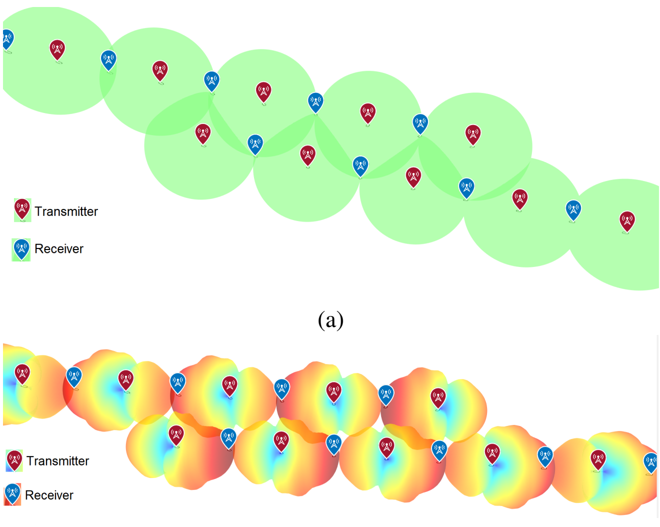

Fig. 6: Radio waves radiation pattern: (a) isotropic transmission and reception; (b) directional transmission and reception with beamforming.

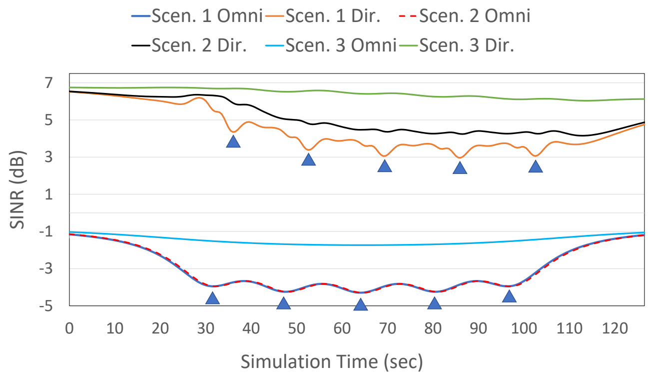

Fig. 7: SINR comparison of employing directional and isotropic antennas for three UAV drone corridor scenarios.

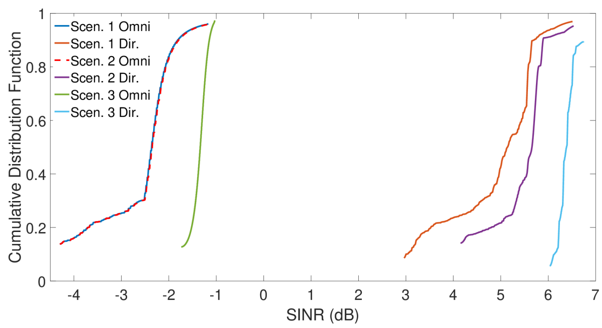

Fig. 8: CDF of the obtained SINR values.

SINR of all three scenarios with the same antenna type. The data collected in Scenario 1 with the beamforming antenna has pronounced SINR variance and a sharp decrease and subsequent increase as drones in the opposing corridor pass through the beam. The points in time when two drones pass each other are indicated by the blue triangles in the figure. These variances are also present in the other scenarios however they appear less pronounced.

This difference is due to the experiment design itself as Scenario 1 has drones passing in the closest horizontal proximity of all of the scenarios considered. The SINR curves obtained from Scenario 3 where the two corridors are three hundred meters apart are the smoothest. The beamforming antenna run of this scenario compared to the same scenario with the isotropic antenna demonstrates that there is an improvement in SINR even when only one drone corridor is present. Overall across all three of the simulated scenarios there was an increase in SINR when using aerial beamforming antennas as compared to their isotropic counterparts. The average SINR for Scenario 1 improved from -3.09 dB to 4.46 dB for the isotropic and beamforming antennas, respectively. Similarly, in Scenario 2 the average SINR improved from -3.09 dB to 5.08 dB. Finally, in Scenario 3, where the corridors are spaced widely apart so that there is little interaction between the two, the average SINR increased from -1.47 dB to 6.43 dB.

Fig. 8 demonstrates the cumulative distribution function (CDF) of the SINR data. Along the x axis we present the given SINR values where the y axis captures the probability of that value occurring in the range given. It also demonstrates that there is a higher probability of a higher SINR when comparing the isotropic antenna to its beamforming counterpart. The large separation between the groups of lines indicates that there is a clear advantage, from an interference mitigation standpoint, to use aerial beamforming antennas compared to standard isotropic antennas.

VI. Conclusion

This paper investigates interference mitigation in clustered groups of UAVs communicating through 5G NR V2X Mode 2. Analytical work demonstrates the advantages of mmWave beamforming for U2U communications. In addition, a real-time simulator leveraging SUMO, NS3, and MATLAB is implemented. The paper presents details about the simulation software, experimental design, and outcomes. Simulation results reveal that mmWave beamforming effectively mitigates interference from transmission collisions among numerous drones flying in close proximity. The paper demonstrates an average SINR increase of 7.88 dB across the three simulated scenarios, offering valuable insights into network performance in drone corridors. These findings prompt further research on aerial communications utilizing microwave or mmWave radio transceivers and different UAV densities.

In the future, we plan to study how to reduce transmission collisions and boost the communication efficiency in dense U2U networks by applying advanced scheduling algorithms [17], [18], or leveraging (physical) network coding network coding [19], [20]. Meanwhile, we will continue to add extra features to the simulator to facilitate a wide array of experiments and verify the proposed principles on the Aerial Experimentation and Research Platform for Advanced Wireless (AERPAW) testbed [21].

Acknowledgment

This work was supported by NSF PAWR program and NSF CCRI program under the grant number CNS-1939334 and 2120442, respectively.

References

[1] G. Oh, Y. Kim, J. Ahn, and H.-L. Choi, "Task allocation of multiple UAVs for cooperative parcel delivery," in *Advances in Aerospace Guidance, Navigation and Control*. Cham: Springer International Publishing, 2018, pp. 443–454.

[2] Y.-J. Chen, *et al.*, "Autonomous tracking using a swarm of UAVs: A constrained multi-agent reinforcement learning approach," *IEEE Trans. Veh. Technol.*, vol. 69, no. 11, pp. 13 702–13 717, 2020.

[3] A. S. Abdalla and V. Marojevic, "Aerial RIS for MU-MISO: Joint base station beamforming and RIS phase shifter optimization," in *2022 IEEE International Conference on Sensing, Communication, and Networking (SECON Workshops)*, 2022, pp. 19–24.

[4] M. Silvagni, A. Tonoli, E. Zenerino, and M. Chiaberge, "Multipurpose uav for search and rescue operations in mountain avalanche events," *Geomatics, Natural Hazards and Risk*, vol. 8, no. 1, p. 18–33, 2016.

[5] A. Bhuyan, I. Guvenc, H. Dai, M. L. Sichitiu, S. Singh, A. Rahmati, S. J. Maeng, E. Ozturk, and M. M. Chowdhury, "Advances in secure 5G network for a nationwide drone corridor," *2022 IEEE Aerospace Conference (AERO)*, 2022.

[6] A. S. Abdalla and V. Marojevic, "Communications standards for unmanned aircraft systems: The 3GPP perspective and research drivers," *IEEE Commun. Standards Mag.*, vol. 5, no. 1, pp. 70–77, March 2021.

[7] *Application layer support for Vehicle-to-Everything (V2X) services*, 3GPP, 4 2020, v16.4.0.

[8] *Third Generation Partnership Project; Technical Specification Group SA; Technical Specification Group Services and System Aspects; Study on supporting Unmanned Aerial Systems (UAS) connectivity, Identification and tracking (Release 17)*, 3GPP, 3 2021, v17.1.0.

[9] *Third Generation Partnership Project; Technical Specification Group Services and System Aspects; Study on application layer support for Unmanned Aerial Systems (UAS); (Release 17)*, 3GPP, 1 2021, v17.1.0.

[10] Y. Zeng, J. Lyu, and R. Zhang, "Cellular-connected UAV: Potential, challenges, and promising technologies," *IEEE Wireless Commun.*, vol. 26, no. 1, pp. 120–127, Jan. 2019.

[11] "IEEE Draft Standard for Aerial Communications and Networking Standards," *IEEE P1920.1/D4*, pp. 1–85, Aug. 2020.

[12] S. Singh, U. Bhattacherjee, E. Ozturk, I. Guvenc, H. Dai, M. Sichitiu, and A. Bhuyan, "Placement of mmwave base stations for serving urban drone corridors," *2021 IEEE 93rd Vehicular Technology Conference (VTC2021-Spring)*, 2021.

[13] Y. Shi, R. Enami, J. Wensowitch, and J. Camp, "UABeam: UAV-based beamforming system analysis with in-field air-to-ground channels," in *2018 15th Annual IEEE International Conference on Sensing, Communication, and Networking (SECON)*, 2018, pp. 1–9.

[14] A. Al-Hourani, S. Kandeepan, and A. Jamalipour, "Modeling air-to-ground path loss for low altitude platforms in urban environments," in *2014 IEEE Global Communications Conference*, 2014, pp. 2898–2904.

[15] A. Nabil, K. Kaur, C. Dietrich, and V. Marojevic, "Performance analysis of sensing-based semi-persistent scheduling in C-V2X networks," in *Proc. IEEE VTC-Fall*, 2018, pp. 1–5.

[16] *Third Generation Partnership Project; Technical Specification Group Radio Access Network; Study on evaluation methodology of new Vehicle-to-Everything (V2X) use cases for LTE and NR; (Release 15)*, 3GPP, 6 2019, v17.1.0.

[17] M. Zhang, Y. Dou, V. Marojevic, P. H. J. Chong, and H. C. B. Chan, "FAQ: A fuzzy-logic-assisted Q learning model for resource allocation in 6G V2X," *IEEE Internet of Things Journal*, vol. Early Access, 2023.

[18] M. Zhang, A. Kumar, P. H. J. Chong, H. C. B. Chan, and B.-C. Seet, "Resource allocation based performance analysis for 5G vehicular networks in urban areas," in *2020 IEEE Wireless Communications and Networking Conference Workshops (WCNCW)*, 2020, pp. 1–6.

[19] M. Zhang, H. Li, F. Chen, H. Hou, H. An, W. Wang, and J. Huang, "A general co/decoder of network coding in hdl," in *2011 International Symposium on Networking Coding*, 2011, pp. 1–5.

[20] M. Zhang, L. Lu, and S. C. Liew, "An optimal decoding strategy for physical-layer network coding over multipath fading channels," *IEEE Transactions on Vehicular Technology*, vol. 64, no. 9, pp. 4365–4372, 2015.

[21] K. Powell, A. S. Abdalla, D. Brennan, V. Marojevic, R. M. Barts, A. Panicker, O. Ozdemir, and I. Guvenc, "Software radios for unmanned aerial systems," in *Proc. 1st International Workshop on Open Software Defined Wireless Networks (OpenWireless'20)*. New York, NY, USA: Association for Computing Machinery, 2020, p. 14–20.